Electronic Supplementary Material (ESI) for Journal of Materials Chemistry C.

Formate-mediated Magnetic Superexchange in the Model Hybrid Perovskite $[(CH_3)_2NH_2]Cu(HCOO)_3$

Rebecca Scatena,*[a] Roger D. Johnson,[b] Pascal Manuel[c] and Piero Macchi[d,e]

[a] Department of Physics, Clarendon Laboratory, University of Oxford, Parks Road, Oxford, OX1 3PU, United Kingdom
[b] Department of Physics and Astronomy, University College London, Gower Street, London, WC1E 6BT, United Kingdom
[c] ISIS Pulsed Neutron and Muon Facility, STFC Rutherford Appleton Laboratory, Chilton, Oxfordshire OX11 0QX, United Kingdom
[d] Department of Chemistry, Materials, and Chemical Engineering, Polytechnic of Milan, Milan 20131, Italy
[e] Istituto Italiano di Tecnologia, Center for Nano Science and Technology CNST@polimi, Milan 20133, Italy

Supporting Information

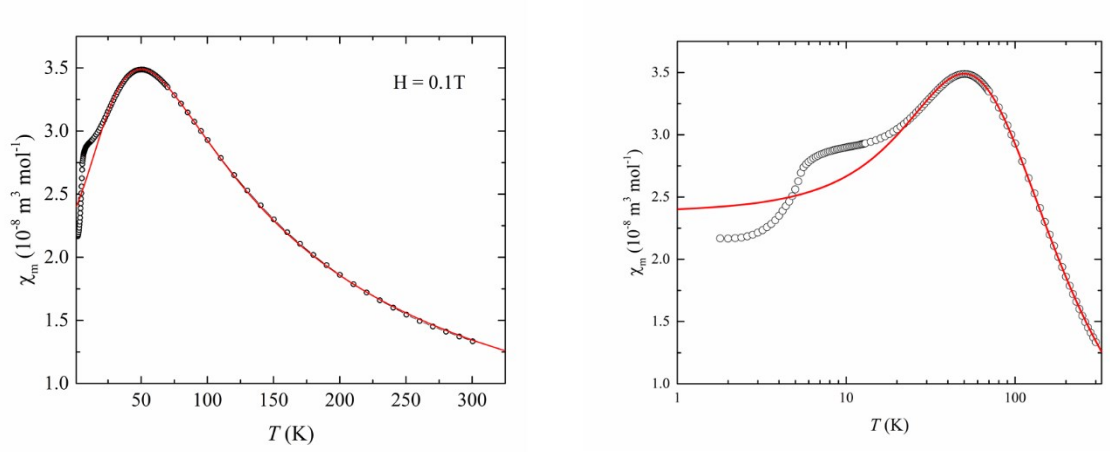

Figure S1. Left: Temperature dependent magnetic susceptibility for a polycrystalline sample of $[Cu(HCOO)_3]H_2N(CH_3)_2$. Right: Zoom-in about the magnetic phase transition. Red profile shows a 1D spin ½ Heisenberg antiferromagnetic correlation.

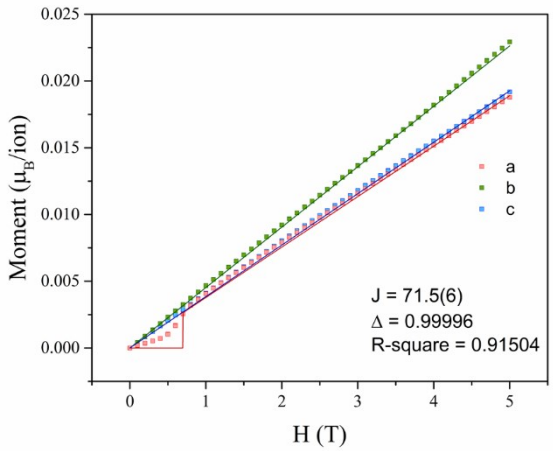

Figure S2. Magnetisation as a function of magnetic field applied along the principal crystallographic axis for a single crystal of $[(CH_3)_2NH_2]Cu(HCOO)_3$ at 2.0 K and minimal model fitting of the linear dependence, see details in the main manuscipt.

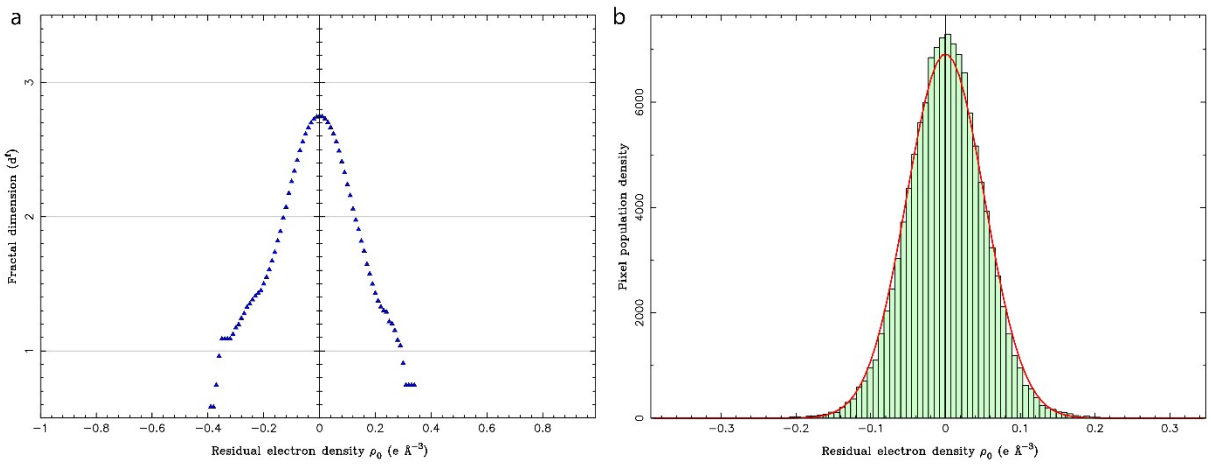

Figure S3. Statistics of residual density distribution for charge density modelling: a) fractal dimension plot and b) probability distribution histogram of residuals for the charge density model.

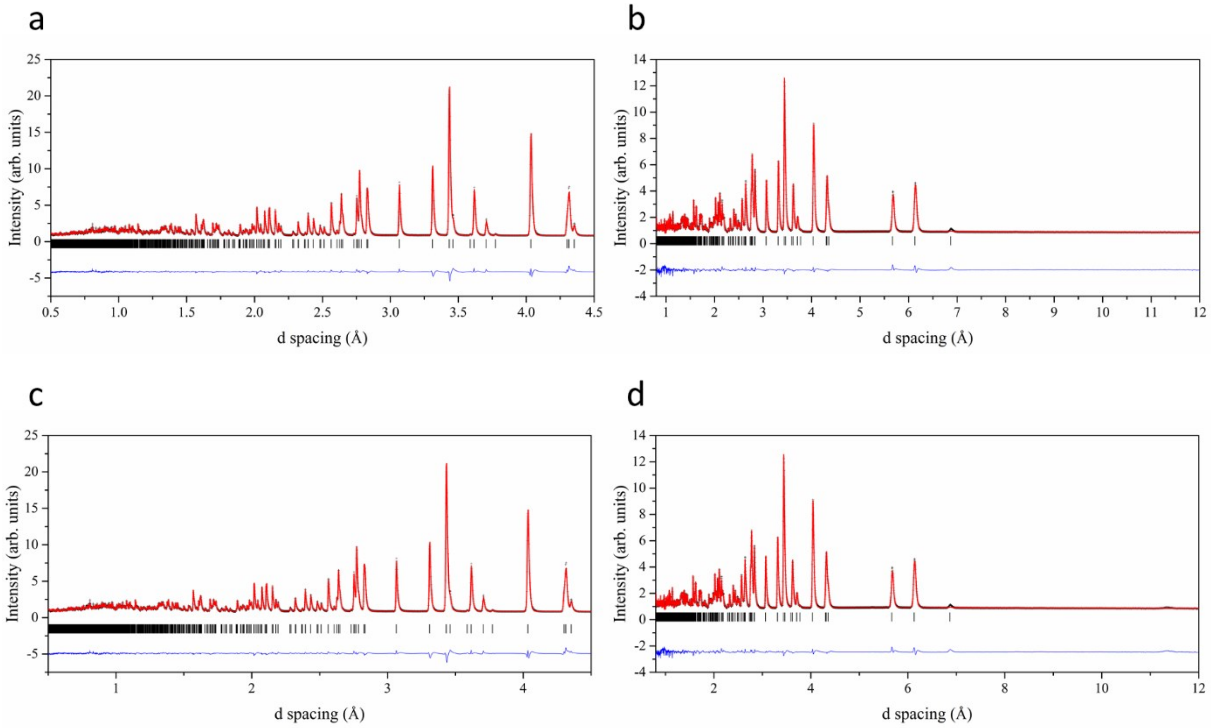

Figure S4. Neutron powder diffraction pattern at T = 10 K (a-b) and T = 1.5 K for $[Cu(DCOO)_3]D_2N(CD_3)_2$. Data and fit are shown as black crosses and a red line, respectively, and their difference is drawn as a blue line. The tick marks show possible Bragg reflection positions for the monoclinic $I2/a$ $[Cu(DCOO)_3]D_2N(CD_3)_2$ phase (first row).

Table S1. Refined Structural Parameter for $[(CH_3)_2NH_2]Cu(HCOO)_3$ from single crystal x-ray diffraction at 110 K and Time-of-Flight Neutron Powder Diffraction Data (used *d*-space range: 0.4 – 12 Å) at 10 K and 1.5 K.

T (K)		110	10	1.5
Crystal system		monoclinic	monoclinic	monoclinic
Space group		*I*2/*a*	*I*2/*a*	*I*2/*a*
a (Å)		8.7835(1)	8.74679(8)	8.74675(8)
b (Å)		8.6468(1)	8.63208(9)	8.63205(9)
c (Å)		11.3974(1)	11.38748(14)	11.38743(14)
β (°)		95.501(1)	95.24689(75)	95.24707(75)
V (Å^3)		861.636(2)	856.186(16)	856.175(16)
Cu(4*d*)	*B* (Å^2)		0.167(87)	0.156(87)
O1(8*f*)	*x, y, z*	0.25787(2), 0.35615(2), 0.597452(16)	0.25735(35), 0.35900(38), 0.09739(25)	0.25734(35), 0.35900(39), 0.09740(25)
	B (Å^2)		0.451(86)	0.456(86)
C1(4*e*)	*y*	0.28769(2)	0.29079(62)	0.29079(62)
	B (Å^2)		0.569(127)	0.565(128)
D1(4*e*)	*y*	0.165(3)	0.15879(72)	0.15883(72)
	B (Å^2)		1.791(130)	1.768(130)
O2(8*f*)	*x, y, z*	0.05043(2), 0.16370(2), 0.689269(17)	0.44963(33), 0.33316(36), 0.30886(28)	0.44964(33), 0.33315(36), 0.30885(28)
	B (Å^2)		0.360(84)	0.358(84)
O3 (8*f*)	*x, y, z*	-0.12903(3), -0.01749(3), 0.67738(2)	0.63258(35), 0.52102(34), 0.32453(30)	0.63252(35), 0.52101(34), 0.32454(30)
	B (Å^2)		0.455(85)	0.453(85)
C2(8*f*)	*x, y, z*	-0.00449(2), 0.037034(18), 0.720932(14)	0.50555(35), 0.45976(38), 0.28357(29)	0.50554(35), 0.45976(38), 0.28354(29)
	B (Å^2)		0.752(89)	0.754(89)
D2(8*f*)	*x, y, z*	0.0617(15), -0.0281(13), 0.7897(12)	0.43756(32), 0.53063(41), 0.21313(28)	0.43758(32), 0.53063(41), 0.21312(28)
	B (Å^2)		1.644(96)	1.643(96)
N1(4*e*)	*y*	0.18549(2)	-0.18637(44)	-0.18637(44)
	B (Å^2)		0.725(90)	0.723(90)
C3(8*f*)	*x, y, z*	-0.13693(3), 0.28106(3), 0.44426(2)	0.13343(42), -0.28592(44), 0.05255(35)	0.13341(42), -0.28590(44), 0.05253(35)
	B (Å^2)		1.035(83)	1.027(83)
D3(8*f*)	*x, y, z*	-0.1979(17), 0.3528(19), 0.3800(15)	0.05516(32), -0.20670(41), 0.09188(24)	0.05517(32), -0.20669(41), 0.09188(24)
	B (Å^2)		1.675(94)	1.663(94)
D4(8*f*)	*x, y, z*	-0.0793(18), 0.3517(19), 0.5112(14)	0.19562(34), -0.35272(47), 0.12190(29)	0.19564(34), -0.35274(47), 0.12188(29)
	B (Å^2)		1.545(97)	1.549(97)
D5(8*f*)	*x, y, z*	-0.0534(19), 0.2032(17), 0.4060(14)	0.07378(35), -0.36171(39), -0.01241(28)	0.07379(35), -0.36169(39), -0.01241(28)
	B (Å^2)		2.217(96)	2.219(96)
D6/H6 (8*f*)	*x, y, z*	-0.1939(19), 0.1157(18), 0.5653(16)	0.19541(51), -0.11411(54), -0.06414(43)	0.19547(51), -0.11413(54), -0.06413(43)
	B (Å^2)		2.589(150)	2.577(150)
	g		0.818(5)/0.182(5)	0.818(0)/0.182(0)
		r_{int} 3.09 %	R_{wp} 2.92 %	R_{wp} 2.94 %
		GOF *w* 1.15	R_p 3.02 %	R_p 3.07 %
		R_1 (F) [I ≥2σ] 1.35 %	R_F 3.44 %	R_F 3.43 %

Table S2. Bond lengths in $[Cu(HCOO)_3]H_2N(CH_3)_2$ refined at T = 110, 10 and 1.5 K from single crystal X-ray and Neutron powder diffraction data. The atomic labels refer to the those reported in the corresponding structural cif files.

T (K)	110	10	1.5
Source	X-ray	Neutron	Neutron
Cu-O1 (Å)	1.97312(19)	1.982(4)	1.982(4)
Cu-O2 (Å)	1.96877(18)	1.949(3)	1.949(3)
Cu-O3 (Å)	2.4545(3)	2.417(3)	2.417(3)
C1-O1(Å)	1.2546(2)	1.252(5)	1.252(5)
C1-H1/D1(Å)	1.06(3)	1.139(8)	1.139(8)
C2-O2(Å)	1.2633(3)	1.242(5)	1.242(5)
C2-O3(Å)	1.2495(4)	1.280(5)	1.279(5)
C2-H2/D2(Å)	1.087(13)	1.133(5)	1.132(5)
C3-N1(Å)	1.4811(3)	1.499(5)	1.499(5)
C3-H3/D3(Å)	1.064(16)	1.092(5)	1.092(5)
C3-H4/D4(Å)	1.066(16)	1.084(6)	1.084(6)
C3-H5/D5(Å)	1.115(17)	1.084(6)	1.084(6)
N3-H6/D6(Å)	1.044(17)	1.042(5)	1.042(5)

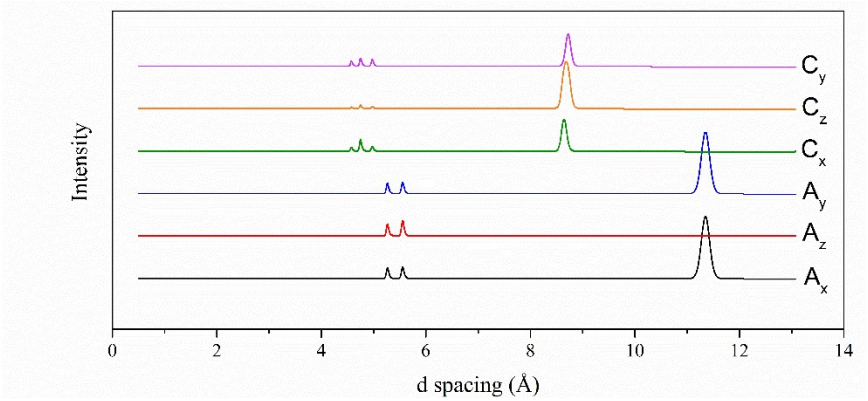

Figure S5. Simulation of the neutron diffraction pattern for all possible magnetic structures allowed by the symmetry of the system given propagation vector (0,0,1).

Table S3. QTAIM integrated charges from experimental multipolar model (Exp. MM) and multipolar model refined against a calculated structure factor (Calc. MM) for $[Cu(HCOO)_3]H_2N(CH_3)_2$.

	Exp. MM		Calc. MM	
	atomic	ionic		
Cu^{2+}	+0.969	+0.969	+0.816	+0.816
$O1^{2-}$	-1.176		-1.036	
C1	+1.825	-0.340	+1.456	-0.571
H1	+0.187		+0.044	
$O2^{2-}$	-1.326		-1.048	
$O3^{2-}$	-1.184	-0.811	-1.018	-0.585
C2	+1.541		+1.433	
H2	+0.158		+0.049	
C3	+0.165		+0.328	
H3	+0.119		+0.049	
H4	+0.105	+1.032	+0.057	+0.956
H5	+0.177		+0.032	
N1	+0.489		+0.470	
H6	-1.076		-0.917	